Rev. Roum. Sci. Techn.– Électrotechn. et Énerg.
Vol. **61**, *3*, pp. 239–243, Bucarest, 2016

NEURAL NETWORK AND FUZZY LOGIC DIRECT TORQUE CONTROL OF SENSORLESS DOUBLE STAR SYNCHRONOUS MACHINE

ELAKHDAR BENYOUSSEF[1], ABDELKADER MEROUFEL[2], SAID BARKAT[3]

Key words: Double star synchronous machine, Multilevel inverter, Direct torque control (DTC), Fuzzy logic control, Neural network, Luenberger observer.

This work relates to the study of direct torque control is applied for salient-pole double star synchronous machine. The machine is supplied by two three-level inverters. Two control approaches using fuzzy logic DTC, and neural network DTC are proposed and compared. The validity of the proposed controls scheme is verified by simulation tests of a double star synchronous machine. The stator flux, torque, and speed are determined and compared in the above techniques. For achieving high performances control of the multiphase drive, the proposed controls method needs accurate information about rotor position and rotor speed. To this end, they are estimated by using Luenberger observer.

1. INTRODUCTION

Multiphase machines have been studied for a long time, but recently they have gained attention in the research community and industry worldwide [1]. Multiphase machines are perceived to offer many advantages such as improved magneto-motive force waveforms, reduced line voltages and increased efficiencies. The consequential benefits of these are reduced torque pulsations, lower losses, reduced acoustic noise and reduced power ratings of supply converters [2, 3].

Among the multiphase machines, five-phase and six-phase induction or synchronous machines are the most considered in the literature. The present study is focused on the double star synchronous machine (DSSM) [4]. Normally two two-level inverters are indispensable for double star electrical drives.

Multilevel converters offer an approach to solve these problems. In this kind of converters, the output voltage can take several discrete levels of equal magnitude. The multilevel inverter, first proposed in [5, 6], was aimed to reduce the harmonic content of generated voltage and current waveforms. If compared with a two-level waveform, the harmonic content of such a waveform is greatly reduced.

The conventional DTC is characterized by its good dynamic performances and robustness [6]. One more significant disadvantage of conventional DTC is ripples, which exists in the torque and flux variables. In the aim to improve the performance of the electrical drives based on DTC, fuzzy logic direct torque control (FLDTC) and neural network direct torque control (DTC-ANN) attracts more and more the attention of many scientists [7, 8].

The elimination of the speed sensor reduces the hardware complexity, size and cost, and increases the reliability of the drive system. Several speed sensorless control schemes have been suggested in literature [9, 10] in order to eliminate the speed sensor. In this work a simple approach based on extended filter observer is adopted, this observer is known by its futures such as order reduction control, and simple hard implementation. This paper is devoted to FLDTC and DTC-ANN of sensorless DSSM using Luenberger observer fed by two three-level neutral-point-clamped (NPC) inverters.

2. DOUBLE STAR SYNCHRONOUS MACHINE MODEL

The stator voltages equations are given by:

$$\begin{cases} v_{s_1} = R_{s_1} i_{s_1} + \mathrm{d}\phi_{s_1} \\ v_{s_2} = R_{s_2} i_{s_2} + \mathrm{d}\phi_{s_2} \end{cases}, \tag{1}$$

with v_{s1}, v_{s2} – stator voltages; i_{s1}, i_{s2} – stator currents; ϕ_{s_1}, ϕ_{s_2} – stator flux.

The transformation of the system six phases to the system (α,β) is given by:

$$\lfloor X_\alpha \quad X_\beta \rfloor = [A] \lfloor X_{s_1} \quad X_{s_2} \rfloor, \tag{2}$$

where: X_{s1} and X_{s2} can represent the stator currents, stator flux, and stator voltages.

The transformation matrix A is given by:

$$[A] = \frac{1}{\sqrt{3}} \begin{pmatrix} 1 & -\frac{1}{2} & -\frac{1}{2} & \frac{\sqrt{3}}{2} & -\frac{\sqrt{3}}{2} & 0 \\ 0 & \frac{\sqrt{3}}{2} & -\frac{\sqrt{3}}{2} & \frac{1}{2} & \frac{1}{2} & -1 \\ 1 & -\frac{1}{2} & -\frac{1}{2} & -\frac{\sqrt{3}}{2} & \frac{\sqrt{3}}{2} & 0 \\ 0 & -\frac{\sqrt{3}}{2} & \frac{\sqrt{3}}{2} & \frac{1}{2} & \frac{1}{2} & -1 \\ 1 & 1 & 1 & 0 & 0 & 0 \\ 0 & 0 & 0 & 1 & 1 & 1 \end{pmatrix}. \tag{3}$$

To express the stator equations in the same reference frame, the following rotation transformation is adopted.

$$P(\theta) = \begin{pmatrix} \cos(\theta) & \sin(\theta) \\ -\sin(\theta) & \cos(\theta) \end{pmatrix}. \tag{4}$$

3. THREE-LEVEL INVERTER MODELING

The three-level NPC inverter consists of twelve pairs of transistors-diodes and six clamping diodes. The simple voltage of each phase is entirely defined by the state of the

[1] University of Kasdi Merbah, Faculty of Science Applied, Department of Electrical Engineering, Ouargla 30000, Algeria
[1,2] Intelligent Control Electronic Power System laboratory, UDL, Sidi Bel Abbes 22000, BP 89 Algeria
[3] University of M'sila, Faculty of Technology, Department of Electrical Engineering, M'sila 28000, BP 166 Algeria

four transistors constituting each arm. The median diodes of each arm permits to have the zero level of the inverter output voltage [5]. Only three sequences of operation are retained and done in work. Each arm of the inverter is modeled by a perfect switch with three positions (0, 1, and 2).

The space vector diagram of a three-level inverter is shown in Fig. 1.

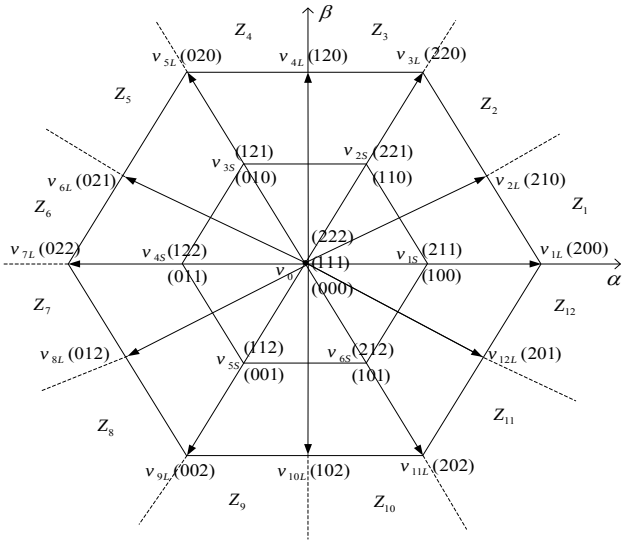

Fig. 1 – Space vector diagram of three-level inverter.

4. **FUZZY LOGIC DIRECT TORQUE CONTROL**

The stator flux is estimated from the measure of stator current and voltage and their transformation in the α-β subspace. The components of stator flux can be estimated by

$$\begin{cases} \hat{\phi}_\alpha(t) = \int_0^t (\hat{v}_\alpha - R_\alpha i_\alpha)\mathrm{d}\tau + \hat{\phi}_\alpha(0) \\ \hat{\phi}_\beta(t) = \int_0^t (\hat{v}_\beta - R_\beta i_\beta)\mathrm{d}\tau + \hat{\phi}_\beta(0) \end{cases}. \quad (5)$$

The stator flux amplitude is given by:

$$\left|\hat{\phi}_s\right| = \sqrt{\hat{\phi}_\alpha^2 + \hat{\phi}_\beta^2}\ . \quad (6)$$

The stator flux angle is calculated by:

$$\hat{\theta}_s = \tan 2^{-1}\left(\frac{\hat{\phi}_\beta}{\hat{\phi}_\beta}\right). \quad (7)$$

Electromagnetic torque equation is given by:

$$\hat{T}_{em} = p\left(\hat{\phi}_\alpha i_\beta - \hat{\phi}_\beta i_\alpha\right). \quad (8)$$

Figure 2 gives the membership functions for input variables E_ϕ, E_T and $\hat{\theta}_s$.

The Luenberger observer will be used to estimate the rotor position and rotor speed of DSSM. The Luenberger observer is based on the error of the actual position and actual speed and their estimated values which must be converged toward zero.

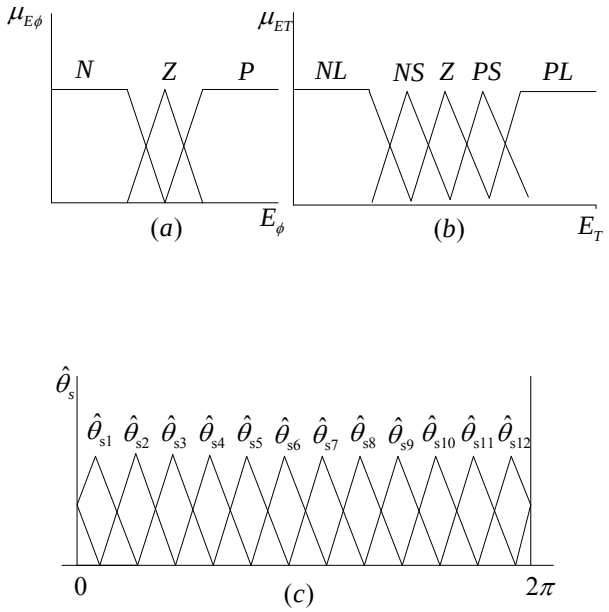

Fig. 2 – Membership functions of input variables: a) flux error; b) torque error; c) stator flux angle.

The Luenberger observer is given by the following system:

$$\begin{cases} \dot{\hat{x}} = A\hat{x} + BU + L(y - \hat{y}) \\ \hat{y} = C\hat{x} \end{cases}, \quad (9)$$

with: $\hat{x} = \left[\hat{\theta} \quad \hat{\Omega} \quad \hat{T}_L\right]^{\mathrm{T}}$, $U = i_q$, $B = \left[0 \quad pM_{fd}i_f/J \quad 0\right]^{\mathrm{T}}$,

$$A = \begin{bmatrix} 0 & p & 0 \\ 0 & -f/J & -1/J \\ 0 & 0 & 0 \end{bmatrix}, C = \begin{bmatrix} 1 & 0 & 0 \\ 0 & 1 & 0 \\ 0 & 0 & 0 \end{bmatrix}, L = \begin{bmatrix} 0 & 0 & 0 \\ l_1 & l_2 & 0 \\ l_3 & 0 & 0 \end{bmatrix}.$$

l_1, l_2, l_3 are the observer gains, T_L is the load torque, i_f is the current of rotor excitation.

This observer can be established from the DSSM model as follows:

$$\begin{cases} \dfrac{\mathrm{d}\hat{\theta}}{\mathrm{d}t} = p\hat{\Omega} \\ \dfrac{\mathrm{d}\hat{\Omega}}{\mathrm{d}t} = \dfrac{1}{J}\left(\hat{T}_{em} - \hat{T}_L\right) - \dfrac{f}{J}\hat{\Omega} + l_1\left(\Omega - \hat{\Omega}\right) + l_2\left(\theta - \hat{\theta}\right) \\ \dfrac{\mathrm{d}\hat{T}_L}{\mathrm{d}t} = l_3\left(\theta - \hat{\theta}\right). \end{cases} \quad (10)$$

The switching tables of the proposed three-level FLDTC are used to select the best output voltage depending on the position of the stator flux and desired action on the torque and stator flux.

The structure of DTC based on fuzzy logic control of sensorless DSSM is shown in Fig. 3.

Table 1

Rules of fuzzy control for first star

$\hat{\theta}_{s1}$				$\hat{\theta}_{s2}$				$\hat{\theta}_{s3}$				$\hat{\theta}_{s4}$			
μ_{ET} \ μ_{Φ}	P	Z	N	μ_{ET} \ μ_{Φ}	P	Z	N		P	Z	N	μ_{ET} \ μ_{Φ}	P	Z	N
PL	v_{3L}	v_{2S}	v_{5L}	PL	v_{3L}	v_{2S}	v_{5L}	PL	v_{5L}	v_{3S}	v_{7L}	PL	v_{5L}	v_{3S}	v_{7L}
PS	v_{2L}	v_{2S}	v_{4L}	PS	v_{4L}	v_{3S}	v_{6L}	PS	v_{4L}	v_{3S}	v_{6L}	PS	v_{6L}	v_{4S}	v_{8L}
ZE	0	0	0	ZE	0	0	0	ZE	0	0	0	ZE	0	0	0
NS	v_{12L}	0	v_{10L}	NS	v_{12L}	0	v_{10L}	NS	v_{2L}	0	v_{12L}	NS	v_{2L}	0	v_{12L}
NL	v_{11L}	v_{5S}	v_{9L}	NL	v_{1L}	v_{6S}	v_{11L}	NL	v_{1L}	v_{6S}	v_{11L}	NL	v_{10L}	v_{1S}	v_{1L}
$\hat{\theta}_{s5}$				$\hat{\theta}_{s6}$				$\hat{\theta}_{s7}$				$\hat{\theta}_{s8}$			
μ_{ET} \ μ_{Φ}	P	Z	N	μ_{ET} \ μ_{Φ}	P	Z	N	μ_{ET} \ μ_{Φ}	P	Z	N	μ_{ET} \ μ_{Φ}	P	Z	N
PL	v_{7L}	v_{4S}	v_{9L}	PL	v_{7L}	v_{4S}	v_{9L}	PL	v_{9L}	v_{5S}	v_{11L}	PL	v_{9L}	v_{5S}	v_{11L}
PS	v_{6L}	v_{4S}	v_{8L}	PS	v_{8L}	v_{5S}	v_{10L}	PS	v_{8L}	v_{5S}	v_{10L}	PS	v_{10L}	v_{6S}	v_{12L}
ZE	0	0	0	ZE	0	0	0	ZE	0	0	0	ZE	0	0	0
NS	v_{4L}	0	v_{2L}	NS	v_{4L}	0	v_{2L}	NS	v_{6L}	0	v_{4L}	NS	v_{6L}	0	v_{4L}
NL	v_{3L}	v_{1S}	v_{1L}	NL	v_{5L}	v_{2S}	v_{3L}	NL	v_{5L}	v_{2S}	v_{3L}	NL	v_{7L}	v_{3S}	v_{5L}
$\hat{\theta}_{s9}$				$\hat{\theta}_{s10}$				$\hat{\theta}_{s11}$				$\hat{\theta}_{s12}$			
μ_{ET} \ μ_{Φ}	P	Z	N	μ_{ET} \ μ_{Φ}	P	Z	N	μ_{ET} \ μ_{Φ}	P	Z	N	μ_{ET} \ μ_{Φ}	P	Z	N
PL	v_{11L}	v_{6S}	v_{1L}	PL	v_{11L}	v_{6S}	v_{1L}	PL	v_{1L}	v_{1S}	v_{3L}	PL	v_{1L}	v_{1S}	v_{3L}
PS	v_{10L}	v_{6S}	v_{12L}	PS	v_{12L}	v_{1S}	v_{2L}	PS	v_{12L}	v_{1S}	v_{2L}	PS	v_{2L}	v_{2S}	v_{4L}
ZE	0	0	0	ZE	0	0	0	ZE	0	0	0	ZE	0	0	0
NS	v_{8L}	0	v_{6L}	NS	v_{8L}	0	v_{6L}	NS	v_{10L}	0	v_{8L}	NS	v_{10L}	0	v_{8L}
NL	v_{7L}	v_{3S}	v_{5L}	NL	v_{9L}	v_{4S}	v_{7L}	NL	v_{9L}	v_{4S}	v_{7L}	NL	v_{11L}	v_{5S}	v_{9L}

Table 2

Rules of fuzzy control for first star

$Star1$	$\hat{\theta}_{s12}$	$\hat{\theta}_{s1}$	$\hat{\theta}_{s2}$	$\hat{\theta}_{s3}$	$\hat{\theta}_{s4}$	$\hat{\theta}_{s5}$	$\hat{\theta}_{s6}$	$\hat{\theta}_{s7}$	$\hat{\theta}_{s8}$	$\hat{\theta}_{s9}$	$\hat{\theta}_{s10}$	$\hat{\theta}_{s11}$
$Star2$	$\hat{\theta}_{s1}$	$\hat{\theta}_{s2}$	$\hat{\theta}_{s3}$	$\hat{\theta}_{s4}$	$\hat{\theta}_{s5}$	$\hat{\theta}_{s6}$	$\hat{\theta}_{s7}$	$\hat{\theta}_{s8}$	$\hat{\theta}_{s9}$	$\hat{\theta}_{s10}$	$\hat{\theta}_{s11}$	$\hat{\theta}_{s12}$

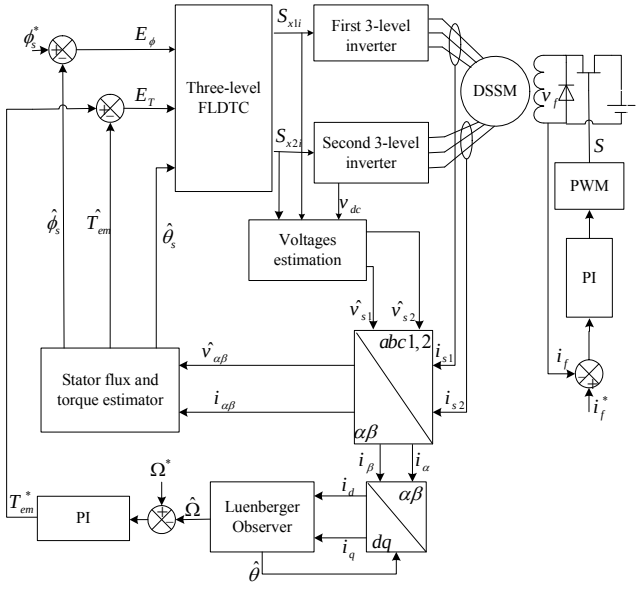

Fig. 3 – Three-level FLDTC scheme for sensorless DSSM (with i = 1, 2, 3 or 4).

5. **NEURAL NETWORK DIRECT TORQUE CONTROL**

The structure of the neural network to perform the DTC applied to DSSM satisfactorily was a neural network with 3 linear input nodes, 12 neurons in the hidden layer (H_1…, H_{12}), and 6 neurons in the output layer [8], as shown in Fig. 4.

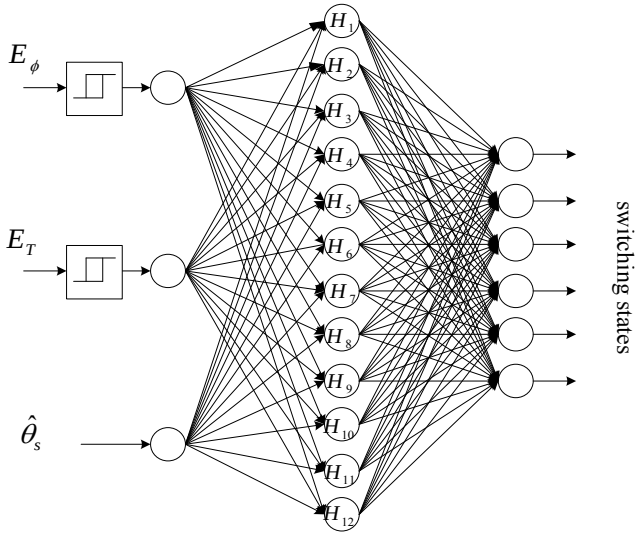

Fig. 4 – Neural network structure for three-level direct torque control.

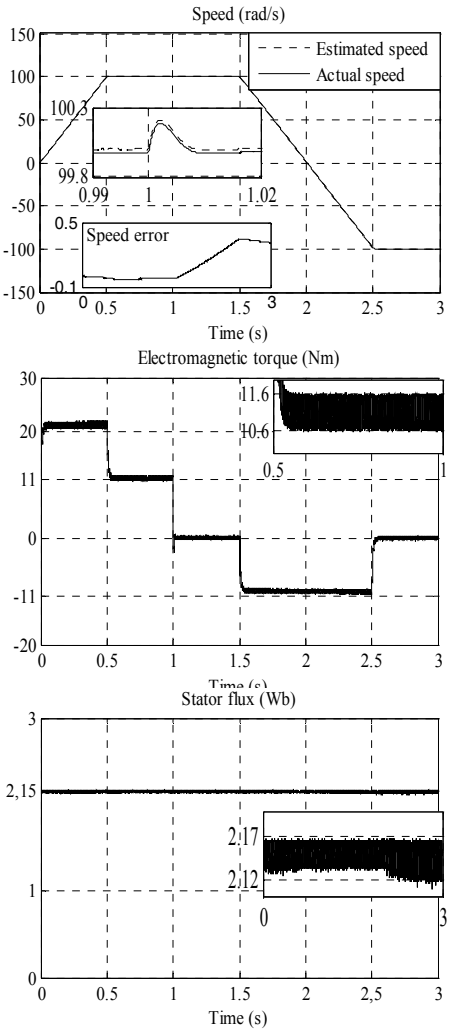

Fig. 5 – Dynamic responses of 3-level FLDTC for sensorless DSSM.

6. **SIMULATION RESULTS**

The observer gains [l_1, l_2, l_3] are chosen as follows: [100 000, 100, 1] to satisfy convergence conditions.

The DSSM is accelerating from standstill to reference speed 100 rad/s. The system is started with full load torque (TL = = 11 N.m). Afterwards, a step variation on the load torque (TL = 0 N.m) is applied at time t = 1 s. And then a sudden reversion in the speed command from 100 rad/s to –100 rad/s was introduced at 1.5 s.

Indeed, Figs. 5 and 6 show the simulation results obtained for the three-level FLDTC and the three-level DTC-ANN of sensorless DSSM respectively. Note that the speed follows its reference value while the electromagnetic torque reaches slowly its reference value. Elimination of the load torque causes a slight variation in speed response. The speed controller intervenes to face this variation and ensures the system follows its suitable reference speed. Moreover, the decoupling control between torque and stator flux is always confirmed.

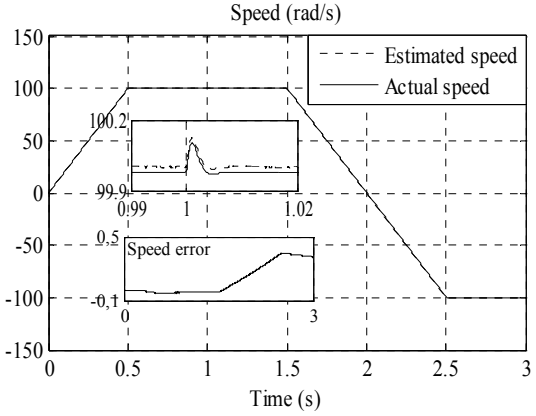

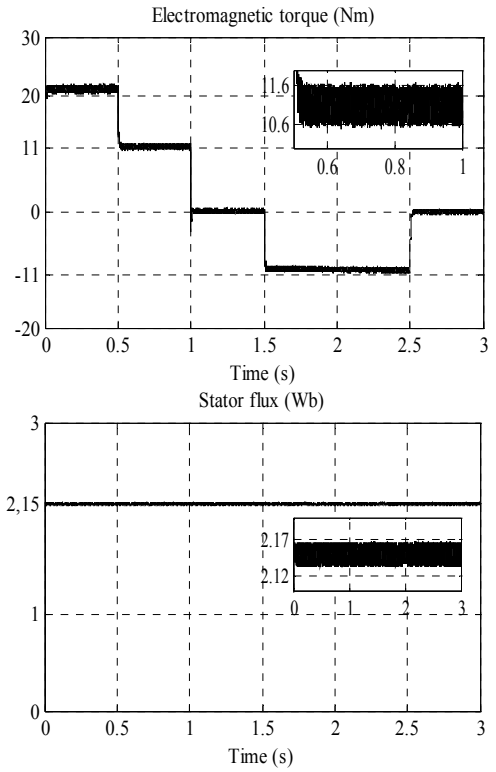

Fig. 6 – Dynamic responses of 3-level DTC-ANN for sensorless DSSM.

It can be observed also that the estimated speed can track the actual speed accurately with minor error. However, the DTC-ANN for sensorless DSSM decreases considerably the flux ripple in comparison with basic FLDTC.

7. **CONCLUSION**

The objective of this work was, at first, to realize an intelligent control system based on DTC applied to a sensorless DSSM fed by two three-level inverters. In the second place, improving dynamic performance; by introducing fuzzy and neural network strategies.

In this paper, one describes mainly the implementation of a law of robust control by presenting a neural network, and fuzzy logic DTC approaches. The simulation results verify that the proposed DTC-ANN scheme achieves a fast torque response and low flux ripple, in comparison to the FLDTC scheme. The decoupling between the flux and the torque is maintained, which confirms the good performances of the developed drive systems. In addition, the simulation results have shown that the proposed sensorless multiphase drive has a satisfactory dynamic response over a wide speed range.

APPENDIX

Table 3

Double star synchronous machine parameters

5 kW, 2 poles, 232 V, 50 Hz	
Components	Rating values
Stator resistance (R_s)	2.35 Ω
Rotor resistance (R_f)	30.3 Ω
d-axis stator inductance (L_d)	0.3811 H
q-axis stator inductance (L_q)	0.211 H
Rotor inductance (L_f)	15 H
Mutual inductance (M_{fd})	2.146 H
Moment of inertia (J)	0.05 Nms^2/rad
Friction coefficient (f)	0.001 Nms/rad

Received on 31 July, 2014

REFERENCES

1. V. Talaeizadeh, R. Kianinezhad, S. Seyfossadat, H. Shayanfar, *Direct Torque Control of Six-Phase Induction Motors Using Three-Phase Matrix Converter*, Energy Conversion and Management, **51**, pp. 2482–2491 (2010).
2. E. Levi *et al*., *Multiphase Electric Machines for Variable Speed Applications*, IEEE Transactions on Industrial Electronics, **55**, *5*, pp. 1893–1909 (2008).
3. G. Aroquiadassou, A. Cavagnino, H. Henao, A. Boglietti, G. Capolino, *A New Circuit Oriented Model for the Analysis of Six-Phase Induction Machine Performances*, Electric Power Systems Research, **78**, pp. 1798–1805 (2008).
4. E. Benyoussef, A. Meroufel, S. Barkat, *Direct Torque Control Using Fuzzy Logic Controller for Double Star Synchronous Machine*, International Conference on Power Electronics and Electrical Drives, Oran, Algeria, 2012.
5. H. Kalpesh, P. Agarwal, *Space Vector Modulation with DC Link Voltage Balancing Control for Three Level Inverters*, International Journal of Recent Trends in Engineering, **1**, *3*, pp. 229–233 (2009).
6. B. Naas, L. Nezli, M. Mahmoudi, M. Elbar, *Direct Torque Control Based Three-Level Inverter Fed Double Star Permanent Magnet Synchronous Machine*, Energy Procedia, **18**, pp. 521–530 (2012).
7. D. Boudana, L. Nezli, A. Tlemcani, M. Mahmoudi, M. Djemai, *DTC Based on Fuzzy Logic Control of a Double Star Synchronous Machine Drive*, Nonlinear Dynamics and Systems Theory, **8**, *3*, pp. 269–286 (2008).
8. F. Kadri, S. Drid, D. Djarah, F. Djeffal, *Direct Torque Control of Induction Motor Fed by Three Phase PWM Inverter Using Fuzzy Logic and Neural Network*, Sixth International Conference on Electrical Engineering, Batna, Algeria, 2010, pp. 12–16.
9. B. Qu, L. Hong, *Design of Sensorless Permanent Magnet Synchronous Motor Control System*, Electronics and Signal Processing, LNEE, **97**, pp. 533–539 (2011).
10. X. Zhuang, M. Rahman, *Comparison of a Sliding Observer and a Kalman Filter for Direct Torque Controlled IPM Synchronous Motor Drives*, IEEE, Transactions on Industrial Electronics, **59**, *11*, pp. 4179–4188 (2012).